Available online at www.sciencedirect.com
ScienceDirect
Progress in Natural Science 18 (2008) 1139–1145
Progress in Natural Science
www.elsevier.com/locate/pnsc

A local geopotential model for implementation of underwater passive navigation

Zhigang Wang *, Shaofeng Bian

Department of Navigation, Naval University of Engineering, Wuhan 430033, China

Received 18 November 2007; received in revised form 17 January 2008; accepted 20 February 2008

Abstract

A main aspect of underwater passive navigation is how to identify the vehicle location on an existing gravity map, and several matching algorithms as ICCP and SITAN are the most prevalent methods that many scholars are using. In this paper, a novel algorithm that is different from matching algorithms for passive navigation is developed. The algorithm implements underwater passive navigation by directly estimating the inertial errors through Kalman filter algorithm, and the key part of this implementation is a Fourier series-based local geopotential model. Firstly, the principle of local geopotential model based on Fourier series is introduced in this paper, thus the discrete gravity anomalies data can be expressed analytically with respect to geographic coordinates to establish the observation equation required in the application of Kalman filter. Whereafter, the indicated gravity anomalies can be gotten by substituting the inertial positions to existing gravity anomalies map. Finally, the classical extended Kalman filter is introduced with the differences between measured gravity and indicated gravity used as observations to optimally estimate the errors of the inertial navigation system (INS). This navigation algorithm is tested on simulated data with encouraging results. Although this algorithm is developed for underwater navigation using gravity data, it is equally applicable to other domains, for example vehicle navigation on magnetic or terrain data.

Keywords: Passive navigation; Fourier series; Local geopotential model; Extended Kalman filter; Inertial navigation system

1. Introduction

Vehicle's underwater passive navigation is an area of research with broad commercial and military application. Recently, there has been greater interest in using geophysical maps (for example gravity) for underwater navigation [1,2], and the main methods that used in map-based navigation are several matching algorithms. These matching algorithms, as Iterative Closest Contour Point (ICCP) and Sandia Inertial Terrain-Aided Navigation (SITAN) algorithm, can bound errors inherent in traditional navigation systems based on dead-reckoning or inertial navigation to a certain extent. ICCP algorithm is a sequence iterative matching algorithm [3–5]; it can give a matching path to correct the indicated path of INS only after getting enough samples, which makes its real-time quality not very good. SITAN algorithm uses a bank of Kalman filters to search the matching position based on information from these Kalman filters recursively [6]. So SITAN is a real-time matching algorithm, but it also wastes a lot of time in the searching procedure and sometimes it gets missed position fixes because of searching points' large quantity.

In this paper, we present an algorithm that is different from matching algorithms for passive navigation. As we all know, vehicle's inertial navigation errors will increase with time going on, and that's why we must make routine adjustment to them. For GPS/INS integrated navigation, with the difference of GPS and INS positions or speeds used

* Corresponding author. Tel.: +86 15926477680; fax: +86 27 83443470.
E-mail address: zswzg1982@sina.com (Z. Wang).

1002-0071/$ - see front matter © 2008 National Natural Science Foundation of China and Chinese Academy of Sciences. Published by Elsevier Limited and Science in China Press. All rights reserved.
doi:10.1016/j.pnsc.2008.02.011

as observations, the INS errors can be optimally estimated through Kalman filtering algorithm to bound the increasing errors. However, for the gravity passive navigation, the available measurements are gravity data only, in this case if some observation equations that contain inertial navigation errors can be obtained, then through Kalman filtering algorithm, the INS errors can also be estimated, and this is the key idea of our algorithm introduced in this paper. To implement this idea we introduced a local geopotential model, and the use of this model in gravity passive navigation will illustrate in full in the following parts of this paper.

2. Principle of gravity passive navigation

The configuration of our passive navigation algorithm is shown in Fig. 1. As indicated, the marine gravimeter provides the measured gravity anomalies that sampled at the vehicle's actual position. Then we find those we name indicated gravity anomalies on map according to INS indicated positions. Subtracting this indicated gravity anomalies from the measured gravity anomalies the observations containing INS position errors are achieved. The local geopotential model is a key part of our algorithm, through which gravity data can be expressed as an analytical equation, and this operation is indispensable to Kalman filtering algorithm to be used as an observation equation. At the existence of observation equation, and with the INS error equations used as state equations, the unknown INS position errors can be estimated eventually on extended Kalman filter algorithm, and thus correct.

There is an issue we must remind the reader, as the measured gravity data are measured at a level surface underwater which is different from the sea surface of gravity map data, in this case a reduction operation [7,8] should be applied to these measured gravity to put them to the same level surface with gravity map. See Refs. [7,8] for the details of reduction operation.

3. The Fourier series-based local geopotential model

To estimate the INS errors on differences between measured and indicated gravity anomalies, it will depend heavily on the analytical relationship between the gravity data and their geographic coordinates, namely the confirmation of geopotential model. Nowadays, most of the popular global geopotential models [9] have reached a high-lever in exponent, and are playing a dominant role in analytically characterizing gravity data. However, these global gravity field models, in essence, are one kind of harmonic analysis under a spherical coordinates system. Due to those complicated Legendre functions with double indexes, when geopotential models with a higher resolution are expected, one faces two-sided difficulties that is the complexity of calculating large quantity Legendre functions and the uncertainty of midband potential coefficients.

Recently, Fast Fourier Transform (FFT) has been extensively investigated by numerous physical geodesists to establish gravity field models for its fast computational speed [10–15]. What the authors feel pity for is that the FFT in physical geodesy is only a discrete form and this makes the models formed by it not suitable for applying in our paper. The gravity field model we use should be an analytical expression like global geopotential model, and at the same time need not to calculate a large number of complex Legendre functions; to fill these two qualifications we consider local geopotential model [16] to be a good choice. With this model the gravity data can be expressed by a continuous Fourier series, and any point of the earth's gravity can be computed once these Fourier coefficients are determined.

3.1. Fourier series expression of local geopotential model

According to [16], the disturbing potential T can be expressed as

$$T(x,y,z)=\frac{1}{2\pi}\int\int\frac{\Delta g(x',y')\,\mathrm{d}x'\,\mathrm{d}y'}{\sqrt{(x'-x)^2+(y'-y)^2+z^2}} \tag{1}$$

Starting from a Laplace's equation in a rectangular coordinates system and making use of a separation variable method, the general solution of Eq. (1) reads

$$T(x,y,z)=\sum\sum\exp(-z\sqrt{n^2w^2+m^2\mu^2})(\cos nwx,\sin nwx)\cdot\begin{pmatrix}A_{nm} & B_{nm}\\ C_{nm} & D_{nm}\end{pmatrix}\begin{pmatrix}\cos m\mu y\\ \sin m\mu y\end{pmatrix} \tag{2}$$

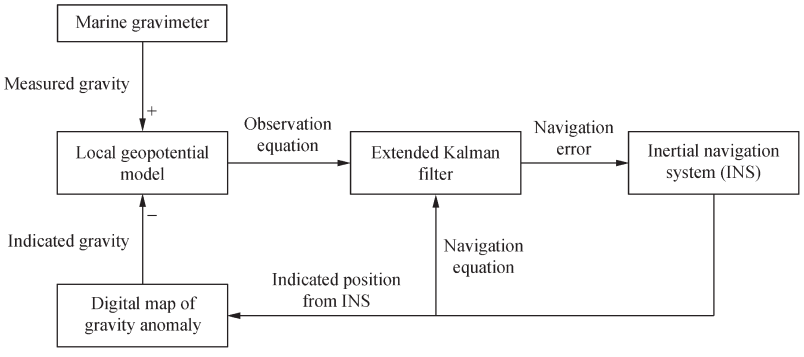

Fig. 1. Sketch of gravity passive navigation algorithm.

where w, μ are circle frequencies, n, m are random non-negative integers, $A_{nm}, B_{nm}, C_{nm}, D_{nm}$ are undetermined coefficients. $\Delta g(x,y)$ is gravity anomaly on sea surface, and x', y' are integration variables.

Assume that gravity anomalies are distributed on the area $\sigma \in [-N < x < N,\ -M < y < M]$ and have been expanded as a two-dimensional Fourier series:

$$\frac{\partial T}{\partial z}|_{z=0} \approx \Delta g(x,y) = \sum\sum(\cos nwx, \sin nwx) \cdot \begin{pmatrix} a_{nm} & b_{nm} \\ c_{nm} & d_{nm} \end{pmatrix} \cdot \begin{pmatrix} \cos m\mu y \\ \sin m\mu y \end{pmatrix} \tag{3}$$

From Eqs. (2) and (3), the following equation can be deduced subsequently:

$$\begin{pmatrix} A_{nm} & B_{nm} \\ C_{nm} & D_{nm} \end{pmatrix} = \frac{1}{\sqrt{n^2w^2 + m^2\mu^2}} \begin{pmatrix} a_{nm} & b_{nm} \\ c_{nm} & d_{nm} \end{pmatrix} \tag{4}$$

where a_{nm}, b_{nm}, c_{nm}, d_{nm} are the Fourier coefficients. According to a two-dimensional Fourier expansion theorem, Eq. (4) holds

$$\begin{pmatrix} a_{nm} & b_{nm} \\ c_{nm} & d_{nm} \end{pmatrix} = \frac{1}{\varepsilon_n \varepsilon_m NM} \int_{-N}^{N}\int_{-M}^{M} \Delta g(x,y) \cdot \begin{pmatrix} \cos nwx \\ \sin nwx \end{pmatrix} \cdot (\cos m\mu y \quad \sin m\mu y)\, \mathrm{d}x\, \mathrm{d}y \tag{5}$$

with

$$\varepsilon_n = \begin{cases} 2, & n = 0 \\ 1, & n \neq 0 \end{cases} \quad \varepsilon_m = \begin{cases} 2, & m = 0 \\ 1, & m \neq 0 \end{cases} \tag{6}$$

$$w = \frac{\pi}{N}, \quad \mu = \frac{\pi}{M} \tag{7}$$

Once the Fourier coefficients are known, inserting Eq. (5) into Eq. (3), the analytical expression of gravity anomaly with respect to latitude and longitude coordinates can be derived. However, there is one issue in this model. That is when we expand gravity anomalies Δg as a two-dimensional Fourier series, gravity anomalies have actually been considered as a periodical function with periodic continuation. This will introduce an additional error of periodical continuation. To significantly reduce this kind of error, the zero padding has been proven as a very effective tool, and when different rate of zero padding (for example, 50%) is adopted, the accuracy of the final result will also be varied. See Ref. [17] for discussion of the effectiveness of the zero padding.

3.2. Numerical analysis of the local geopotential model

According to the theoretical analysis mentioned above, the local geopotential model is one Fourier fitting method in essence. And the fitting accuracy of gravity data to latitude and longitude coordinates directly determines whether it can be applied in passive navigation or not. Once the model accuracy meets our expectation, and considering its analytical expression, then it can be applied in vehicle underwater passive navigation.

To verify the accuracy of this local geopotential model, a numerical computation is carried out on one test area with typical matchable quality. The test area consists of 117×77 gravity anomalies data with a resolution of $2' \times 2'$. The maximum of map data is 180.4364 mGal and the minimum is -235.1216 mGal.

The left panel in Fig. 2 shows contour map of the fitting gravity anomalies by local geopotential model with 50% zero padding. The right panel in Fig. 2 gives the original gravity anomalies. Comparing the fitting gravity anomalies with the original data, we can see that the fitting contours are almost similar to the original ones. Fig. 3 shows the difference between fitting gravity anomalies and the original data, from which we see the high similarity of them. However, there is one problem we must face, that is the "marginal effect". Fig. 3(a) shows that "marginal effect" means fitting errors are large in the margin of the map, and we can see from Fig. 3(a) how serious this effect is, for these numerical values are far from zero. From Fig. 3(b) we can find that the large error points exist only in the margin area of the map (which is very small). So we can discard this error area after applying the model to passive navigation.

Table 1 shows the error statistics of the fitting gravity anomalies and these statistical data are obtained without considering the influence of marginal data, where Δg_m stands for the gravity anomalies on gravity map, Δg_f stands for the fitting gravity anomalies.

From Table 1, one can see that the average error of local geopotential model is 0.1331 mGal only. These results agree with what we expected in the preceding sections, and indicate that with its high degree of accuracy and analytical expression, the local geopotential model is quite adaptive for underwater passive navigation to generate an observation equation.

4. Errors estimation for inertial navigation

4.1. State model

The passive navigation algorithm in this paper utilizes the differences between measured gravity anomalies and indicated gravity anomalies as observations according to Eq. (3), and these observations are nonlinear in their analytical expression. In this case, an extended Kalman filter will be used to process them for their nonlinear expression, since the extended Kalman filter [18,19] is the most popular approach to nonlinear estimation.

The navigation error propagation model in [20] is introduced in this section. The navigation equation is

$$\delta\dot{X}(t) = F(t) \cdot \delta X(t) + G(k) \cdot W(t) \tag{8}$$

in which

$$\delta X(t) = [\delta V_x, \delta V_y, \delta\varphi_i, \delta\lambda_i, \phi_x, \phi_y, \phi_z, \delta A_{xc}, \delta A_{yc}, \varepsilon_{xc}, \varepsilon_{yc}, \varepsilon_{zc}]^{\mathrm{T}}$$

stands for the deviation between actual quantities and INS-indicated values relative to the earth centered/earth fixed

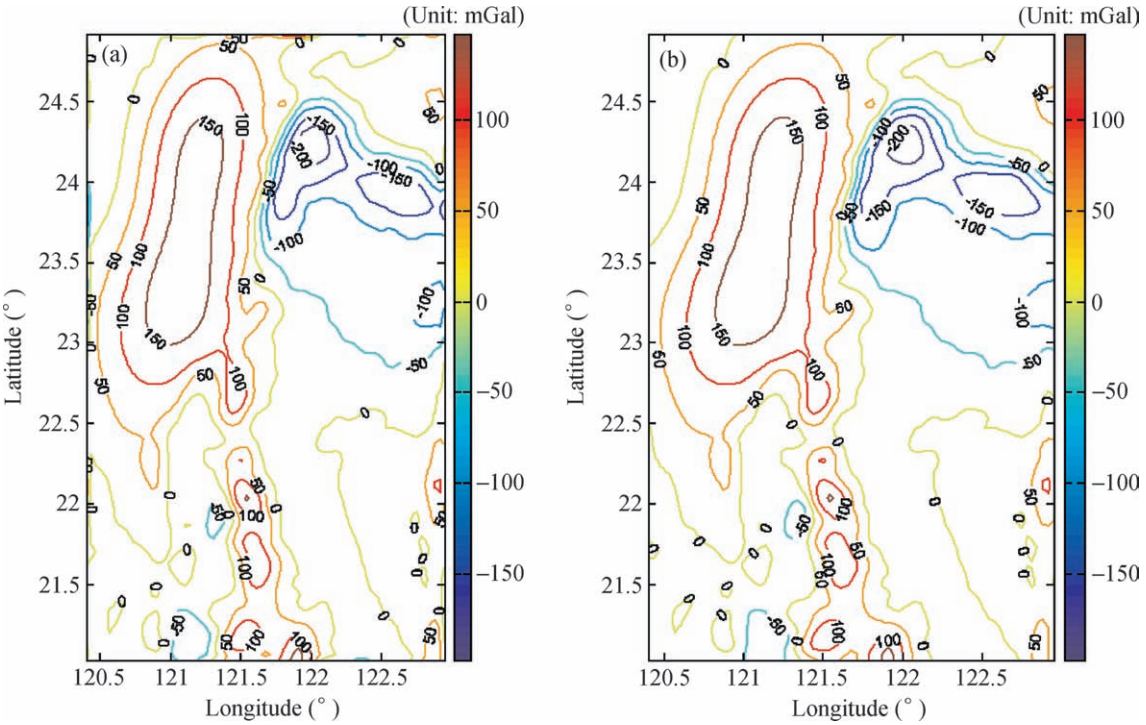

Fig. 2. The fitting and original gravity anomalies. (a) The fitting gravity anomalies; (b) the actual gravity anomalies.

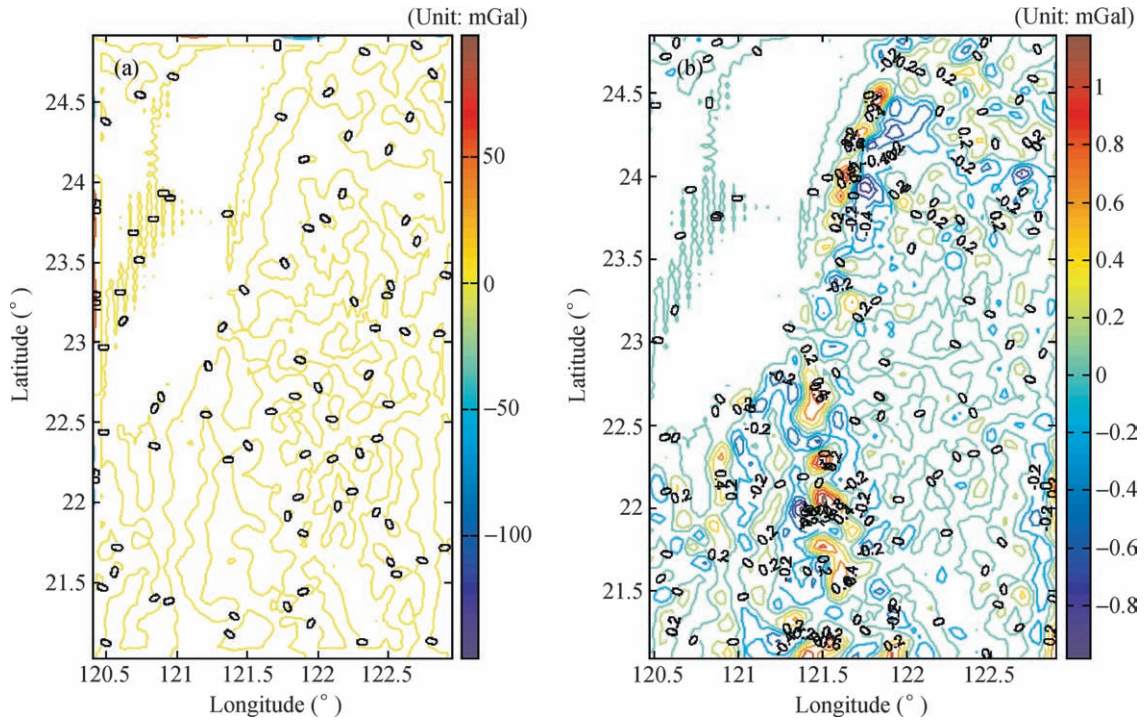

Fig. 3. Fitting errors of gravity anomalies with 50% zero padding. (a) Considering the marginal effect; (b) without considering the marginal effect.

frame. $W(t) = [\delta A_{xs}, \delta A_{ys}, \varepsilon_{xs}, \varepsilon_{ys}, \varepsilon_{zs}]$ is zero-mean, white system noise vector; $F(t)$, the system matrix; $G(k)$, the system control matrix; δV_x and δV_y denote the velocity errors of inertial instrument in latitude and longitude; $\Delta\varphi_i$ and $\Delta\lambda_i$ are the vehicle position errors; ϕ_x, ϕ_y, ϕ_z the roll error, pitch error and heading error, respectively; $\delta A_{xc}, \delta A_{yc}$ are accelerometer constant zero-bias in east and north orientations; $\varepsilon_{xc}, \varepsilon_{yc}, \varepsilon_{zc}$ are gyro constant zero-bias in east, north and azimuth orientation; $\delta A_{xs}, \delta A_{ys}$, the accelerometer ran-

Table 1
Error statistics of local geopotential model (mGal)

Items	Maximum	Minimum	Mean	MSE
$\lvert\Delta g_m - \Delta g_f\rvert$	1.2565	5.0974e−006	0.1331	0.1474

dom zero-bias in east and north orientations; $\varepsilon_{xs}, \varepsilon_{ys}, \varepsilon_{zs}$ are gyro random zero-bias in east, north and azimuth orientations. These variables mentioned above are detailed in [20] or in many standard textbooks on inertial navigation system. Note that the navigation equation is continuous, and a discretization transform should be taken to it, since the extended Kalman filter is only a discrete recursive estimator. Also see [20] for this discretization transform.

The discrete-time navigation equation takes the following form:

$$\delta\dot{X}_{k+1} = F_k \cdot \delta X_k + G_k \cdot W_k, \quad k = 1, \ldots, N \tag{9}$$

where N is the number of samples.

4.2. Observation model

The observable equation is expressed as

$$h = \Delta g(\varphi_t, \lambda_t) - \Delta g(\varphi_i, \lambda_i) \tag{10}$$

where $\Delta g(\varphi_t, \lambda_t)$ is the measured gravity anomaly at the actual vehicle position (φ_t, λ_t) and $\Delta g(\varphi_i, \lambda_i)$ is the gravity anomaly from the map at the indicated position (φ_i, λ_i). Since the equation of h with respect to INS position error is nonlinear, a linear approximation is used in modeling this observable as follows:

$$\begin{aligned} h &\cong [\partial \Delta g(\varphi, \lambda)/\partial\varphi|_{\varphi=\varphi_i}] \cdot \Delta\varphi_i + [\partial \Delta g(\varphi, \lambda)/\partial\lambda|_{\lambda=\lambda_i}] \\ &\quad \cdot \Delta\lambda_i + n \\ &= \Delta g_\varphi|_{\varphi=\varphi_i} \cdot \Delta\varphi_i + \Delta g_\lambda|_{\lambda=\lambda_i} \cdot \Delta\lambda_i + n \end{aligned} \tag{11}$$

where $\Delta\varphi_i$ and $\Delta\lambda_i$ are the inertial position error estimates, and n represents the errors for the measurement and map data. The localized gravity anomaly function $\Delta g(\varphi, \lambda)$ is determined by applying the local geopotential model to discrete gravity anomaly map values in the vicinity of φ and λ. According to Eq. (3) we have

$$\begin{aligned} \Delta g_\varphi|_{\varphi=\varphi_i} &= nu \cdot \sum\sum(-\sin nu\delta(\varphi_i), \cos nu\delta(\varphi_i)) \\ &\quad \cdot \begin{pmatrix} a_{nm} & b_{nm} \\ c_{nm} & d_{nm} \end{pmatrix} \cdot \begin{pmatrix} \cos mv\delta(\lambda_i) \\ \sin mv\delta(\lambda_i) \end{pmatrix} \\ \Delta g_\lambda|_{\lambda=\lambda_i} &= mv \cdot \sum\sum(\cos nu\delta(\varphi_i), \sin nu\delta(\varphi_i)) \\ &\quad \cdot \begin{pmatrix} a_{nm} & b_{nm} \\ c_{nm} & d_{nm} \end{pmatrix} \cdot \begin{pmatrix} -\sin mv\delta(\lambda_i) \\ \cos mv\delta(\lambda_i) \end{pmatrix} \end{aligned}$$

Then we have the discrete-time observation equation

$$h_k \approx \begin{bmatrix} zeros(2,1) \\ \Delta g_\varphi|_{\varphi=\varphi_i} \\ \Delta g_\lambda|_{\lambda=\lambda_i} \\ zeros(8,1) \end{bmatrix}^T \cdot \delta X_k + n_k = H_k \cdot \delta X_k + n_k \tag{12}$$

where H_k is the discrete-time linearized observation matrix, n_k is the discrete-time measurement noise, $zeros(n, m) \in R^n \times R^m$ stands for zero matrix. By now, the INS position errors can be estimated on navigation equation Eq. (9) and observation equation Eq. (12) through the extended Kalman filter.

5. Simulation

In this section, we apply the local geopotential model to underwater passive navigation to estimate the INS errors. Simulation is done on the test area in Section 3.2, the initial position of vehicle is $(21.1^\circ, 122.0^\circ)$ with position error of 2 nmile, the characters of inertial instrument are as shown in Table 2.

The initial angular errors are $\phi_{x_0} = 1$ deg, $\phi_{y_0} = 1$ deg and $\phi_{z_0} = 3$ deg. Before measurements are taken, we assume the initial state vector $\mathbf{X}(0) = \text{zero}(12, 1)$. Nowadays, the dynamic accuracy of marine gravimeter has reached the level of 1 mGal. Moreover, considering the synthetical influence of cross-coupling and Eötvös effect, we assume the noise of gravimeter to be 9 mGal^2. The results of simulation are shown in Figs. 4–6.

Fig. 4 shows the 8-h passive navigation results. The estimated path on gravity anomalies data is curve 3 which consists of 80 samples with a sample interval 0.1 h. The curve 2 is the actual path, while the indicated path is curve 1. The actual path is generated by perturbing the indicated path (obtained from dead-reckoning) with fixing errors. In Fig. 4 we can see that the estimated path matches well with the actual track, which demonstrates the effectiveness of passive navigation algorithm developed in our paper.

Fig. 5 shows the estimation of INS position errors in latitude (Fig. 5(a)) and longitude (Fig. 5(b)), from which we can see that the INS position errors can be estimated perfectly with the local geopotential model used as observation equation. And this result also indicates that it is feasible to extract the position errors contained in differences between measured and indicated gravity anomalies.

Table 2
Characters of inertial instrument

Items	Accelerometers (g)	Gyros (°/h)
Constant bias	1×10^{-4}	0.1
Random bias	5×10^{-5}	0.1

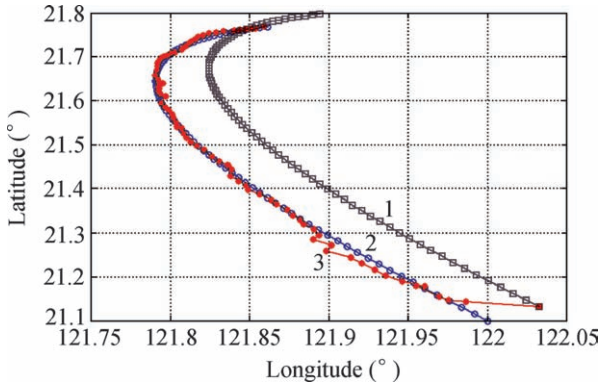

Fig. 4. Simulation result of passive navigation. Curves 1, 2, and 3 represent the indicated path, actual path and estimated path, respectively.

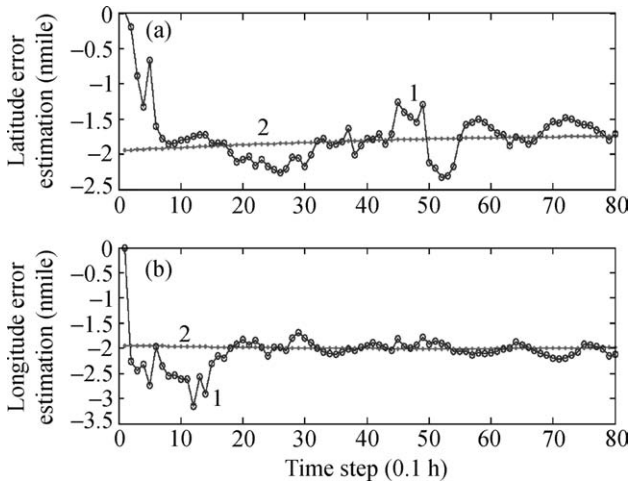

Fig. 5. Estimation of INS position error. (a) Curve 1 represents error estimation with passive navigation in latitude, and curve 2 represents actual error of INS in latitude; (b) curve 1 represents error estimation with passive navigation in longitude, and curve 2 represents actual error of INS in longitude.

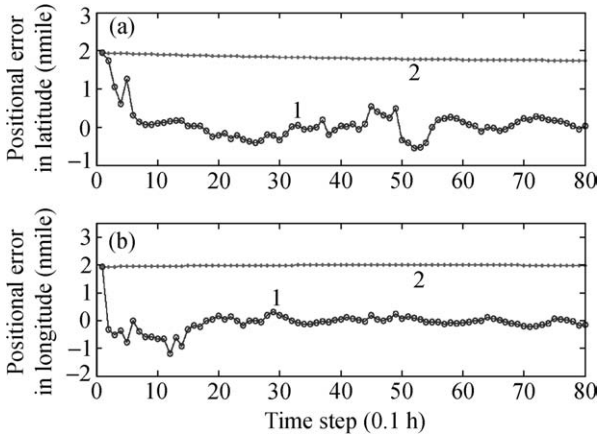

Fig. 6. Positional error of passive navigation. (a) Curve 1 represents positional error of passive navigation in latitude; curve 2 represents positional error of INS in latitude; (b) curve 1 represents positional error of passive navigation in longitude; curve 2 represents positional error of INS in longitude.

Fig. 6, which shows the positional errors of passive navigation in latitude (Fig. 6(a)) and longitude (Fig. 6(b)), demonstrates that the gravity passive navigation can bound the latitude and longitude errors, so reduces these errors growth.

Table 3 is the error statistics, from which we can see the accuracy of the gravity passive navigation.

Table 3
Positional error statistics of gravity passive navigation (nmile)

Items	Maximum	Minimum	Mean	MSE
Error in latitude	1.9440	0.0022	0.2499	0.3304
Error in longitude	1.9653	0.0006	0.1975	0.2964

6. Summary

Underwater gravity passive navigation is an area of research with broad commercial and military applications for it provides accurate navigation without reliance on GPS. The implementation of Kalman filter in gravity passive navigation requires modeling for the gravity observation. In this case a local geopotential model is introduced in our paper to implement this operation. According to our algorithm for passive navigation, the INS errors can be estimated directly without the use of any matching algorithms. The theoretical formulation and numerical investigation in the paper give us an insight that the local geopotential gravity field model has high resolution, and the results of simulation also demonstrate its effectiveness in underwater passive navigation. We believe, with the improvement in marine gravity data resolution the accuracy of this local geopotential model will increase, and the performances of gravity passive navigation can be better improved.

Acknowledgement

This work was supported by National Natural Science Foundation of China (Grant Nos. 40125013 and 40644020).

References

[1] Rice H, Mendelsohn L, Aarons R, et al. Next generation marine precision navigation system. In: Proceedings of IEEE position location and navigation symposium, New York, USA, March 13–16; 2000. p. 13–6.
[2] Moryl J, Rice H, Shinners S. The universal gravity module for enhanced submarine navigation. In: Proceedings of IEEE position location and navigation symposium, New York, USA, April 20–23; 1998. p. 20–3.
[3] Behzad KP, Behrooz KP. Vehicle location on gravity maps. In: Proceedings of SPIE – the international society for optical engineering, Orlando, USA, April; 1999. p. 182–91.
[4] Besl PJ, McKay ND. A method for registration of 3D shapes. IEEE Trans Pattern Anal Mach Intell 1992;14:239–56.
[5] Kamgar-Parsi B. Matching sets of 3D line segments with application to polygonal arc matching. IEEE Trans Pattern Anal Mach Intell 1997;19:1090–9.
[6] Hollowell J. HELI/SITAN: a terrain referenced navigation algorithm for helicopters. In: Proceedings of IEEE position, location, and navigation symposium 1990 (PLANS'90), Las Vegas, NV, USA, March 20–23; 1990. p. 616–25.
[7] Bian SF, Zhang CJ. Computation of topographic effects on vertical gravity gradient. Comput Tech Geophys Geochem Exploration 1999;21(2):133–40.
[8] Bian SF. Some cubature formulas for singular integrals in physical geodesy. J Geodesy 1997;71:443–53.
[9] Heiskanen WA, Morits H. Physical geodesy. 1st ed. San Francisco: W.H. Freeman and Company; 1980, p. 86–93.
[10] Harrison J, Dichison M. Fourier transform and its application in local gravity modeling. Bull Geod 1989;63:149–66.
[11] Harrison J, Dichison M. The Fourier methods in local gravity modelling. Bull Geod 1989;63:149–66.
[12] Bracewell RN. The Fourier Transform and its applications. 2nd ed. New York: McGraw Hill; 1986, p. 58–73.
[13] Brigham EO. The Fast Fourier Transform and its application. 1st ed. New Jersey: Prentice Hall, Englewood Cliffs; 1988, p. 67–75.

[14] Schwarz KP, Sideris GGM, Forsberg R. The use of FFT techniques in physical geodesy. Geophys J Int 1990;100(6):485–514.
[15] Li JC, Ning JS, Chao DB. Several problems in the application of satellite altimetry in physical geodesy. J Wuhan Tech Univ 1996;21(1):9–13, [in Chinese].
[16] Joachim M, Bian SF. Implementing the Fourier series as a local geopotential model in the local gravity field modeling. Anno Lvii-Bollettino Di Geodesia E Scienze Affini 1998;3:293–305.
[17] Tziavos. Comparisons of spectral techniques for geoid computations over large scale. J Geodesy 1996;70:357–73.
[18] Yang YX. Adaptive navigation and kinematic positioning. 1st ed. Beijing: Press of Surveying and Mapping; 2006, p. 45–51 [in Chinese].
[19] Jazwinski AH. Stochastic processes and filtering theory. 1st ed. New York: Academic Press; 1970, p. 36–44.
[20] Farrell JA, Barth M. The global positioning system and inertial navigation. 2nd ed. New York: McGraw-Hill; 1999, p. 123–42.